3D Beamforming for 5G Millimeter Wave Systems Using Singular Value Decomposition and Particle Swarm Optimization Approaches

Osama Alluhaibi, Manish Nair, Amjed Hazzaa[1], Aza Mihbarey[2] and Jiangzhou Wang
School of Engineering and Digital Arts, University of Kent, Canterbury, CT2 7NT, United Kingdom.
[1] College of Engineering, University of Kirkuk, Kirkuk, IRAQ.
[2]Midland Refinery Company, Ministry of Oil, Baghdad, IRAQ.

***Abstract*—Millimeter wave (mmWave) systems are one of the proposed solutions for the fifth generation (5G) mobile network. However, mmWave system experiences strong path loss due to higher frequencies. To solve this problem, such a system demands a narrow beampattern to reduce the loss of the mmWave signal energy due to the high path loss. One of the significant challenges to be addressed before their deployment is designing three dimensional (3D) beamforming algorithms, which are required to be directional. In this paper, we first propose two 3D beamforming algorithms with aim of tracking users in both the azimuth and elevation planes. Our proposed beamforming algorithms operates based on the principles of singular value decomposition (SVD) and particle swarm optimization (PSO). Furthermore, these beamforming algorithms are designed to have limited or negligible side lobes, which cause less interference to the other users operating in the same cell. In order to achieve this objective, Kaiser Bessel (KB) filter is adopted which helps in mitigating side lobes in the synthesized beampattern. Based on our analysis, we gain some valuable insights. The proposed algorithms are shown to perform well in achieving considerable capacity and lower side lobs.**

I. Introduction

Mobile networks have been growing exponentially and have led to scarcity of bandwidth since current mobile communication systems (2G-4G) operate below the 5GHz band [1]–[24]. 90% of the spectrum falls in the millimeter wave (mmWave) band i.e. $>$ 6GHz, qualifying it as one of the viable solutions for future mobile networks [25]. Deployment of mmWave remains a largely unexplored frontier in mobile communication, and many issues are required to be addressed [26]. One of the key issues when designing beamforming algorithms for mmWave is that it experiences strong path loss due to higher frequencies. On the other hand, these higher frequencies allow us to pack a large number of antennas, resulting in strong diversity gains which can overcome the high path loss [27]. Due to this reason, mmWave base stations (BS)s can have massive number of antennas [28]. Scaling up the number of users in practice, however, tracking them by solely using the angle of azimuth becomes impractical in 5G. Therefore, angles of elevation and azimuth will be utilized to track and separate them from one another. Therefore, the three dimensional (3D) beamforming systems have received great interest recently because of the spatial diversity advantage and capability for full-dimensional beamforming, making them promising candidates for practical realization of mmWave systems [19], [27].

Beamforming for planar arrays has been implemented earlier in [29]–[31]. In [29], the 3D beamforming is investigated from the array factor point of view. However, the beamforming weight vector was designed based on elevation angle vector only without exploiting the both angles. To address this issue, researchers in [30]–[32] are designed 3D beamforming weight vectors based on minimum variance distortion (MVD). The MVD approach finds the weight vector in $x-$axes and the weight vector in $y-$axes. Nevertheless, 3D mmWave channel measurements in [33] showed that kronecker product for x and y-axes is required which means a joint xy-axes 3D beamforming weight vectors are demanded. In this case, MVD cannot achieve the optimal solution unless the beamformer weights are independent, which is not this case here because of the kronecker product. In this paper, we propose two new beamforming algorithms with aim of designing joint xy-axes weights vectors. These algorithms utilize both angles of azimuth and elevation to maximize the SNR of the system, unlike other algorithms which maximize the SNR of the system in one dimension [30]–[32]. The propose algorithms work on principle of singular value decomposition (SVD) [34], [35] and particle swarm optimization (PSO). In the first approach, the channel matrix is factorized into singular values which are then used to design the weights of the beamformer. In SVD approach the matrix inversion increases the computational complexity of the system especially when massive number of antennas are allocated in the BS. To reduce the complexity of SVD, a second approach based on PSO is proposed. PSO is a stochastic iterative optimization technique which neither requires any matrix inversion nor any matrix factorization to find the weights of the beamformer.

Moreover, 3D mmWave channel measurements in [33] showed that the effect of side lobs on the beampattern is high which has not been considered in [29]–[31]. In this paper, Kaiser Bessel (KB) filters are designed for the 3D beamforming. The KB filters can reduce the side lobes and make the beam more directional causing less interference to users operating in the same area. The key contributions of the paper are as follows

- We construct two beamforming algorithms for mmWave system which operate on the principles of SVD and PSO.
- Applying KB filtering for reducing the side lobes and improving the directivity of the beampattern.

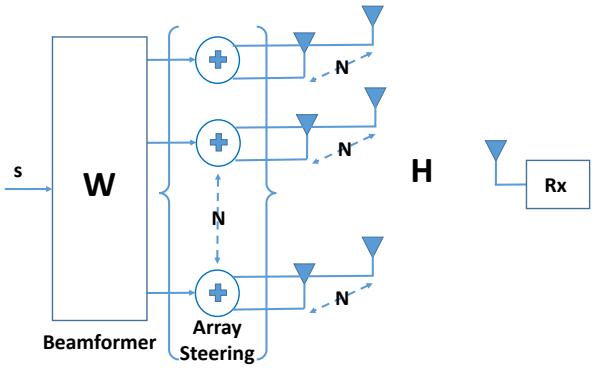

Figure 1: Block diagram of mmWave system

Based on our analysis, we gain some valuable insights. The proposed algorithms are shown to perform well in achieving considerable capacity and lower side lobs.

Notation: Bold upper case letters, $\boldsymbol{X}$, and lower case letters, $\boldsymbol{x}$, denote matrices and vectors, respectively. Transposition and conjugate transposition of a matrix are respectively denoted by $(\cdot)^T$ and $(\cdot)^H$. Determinant of the matrix $\boldsymbol{X}$ is given as $|det(\boldsymbol{X})|$. While, the (m,n)th element of a matrix $\boldsymbol{X}$ is denoted by x_{mn} and mth column vector of a matrix $\boldsymbol{X}$ is denoted by $\boldsymbol{x}_m$. The element wise multiplication is denoted by $\odot$ and the kronecker product is denoted by $\otimes$, respectively.

II. Downlink Communication Model

Consider a system with $N_t = N \times N$ transmitted antennas as shown in Fig. 1. From the figure, it can be observed that a beamformed signal is transmitted by a mmWave BS to a mobile station (MS). Unlike, the two dimension (2D) transmit beamformer, this beamformer will account for both the elevation and azimuth angles. The received signal at the MS in the time domain is given by

$$\boldsymbol{y} = \boldsymbol{HWs} + \boldsymbol{u}, \tag{1}$$

where $\boldsymbol{s}$ is the transmitted data stream drawn from the uniform distribution of equally likely BPSK symbols $[+1,-1]$, having symbol energy E_s at every time slot. $\boldsymbol{H}$ consists of 3D channel, $\boldsymbol{W}$ is the designed beamformer, and $\boldsymbol{u}$ is the complex Gaussian noise vector. Each element of $\boldsymbol{n}$ is modeled as independent and identical distributed (iid) complex Gaussian random variable with zero mean and σ^2 variance of the noise. SNR represents the average SNR per receive antenna, which in this case is expressed as

$$\text{SNR} = \frac{|det[\boldsymbol{H}^H\boldsymbol{W}^H\boldsymbol{WH}]|}{\sigma^2}. \tag{2}$$

As the capacity of the system increase logarithmically with SNR, maximizing SNR will improve the capacity of the system. From (2), it can be observed the SNR is a function of beamformer weights $\boldsymbol{W}$. Our approach is to design a beamformer weight matrix which is of dimension $N \times N$ such that it maximizes the SNR as mentioned in (2). Designing beamforming weights will be covered in detail in upcoming Section III.

A. 3D Channel

Winner II which is a stochastic based geometry model has been considered in this paper [36], [37]. The channel response is given by

$$\begin{aligned}\boldsymbol{H} &= \sqrt{10^{\frac{-PL+\sigma_{SF}}{10}}}\left(\sqrt{\frac{1}{K+1}}\begin{bmatrix}\boldsymbol{a}_x(\phi,\theta)\\ \boldsymbol{a}_y(\phi,\theta)\end{bmatrix}\right.\\ &+ \left.\sqrt{\frac{K}{K+1}}\begin{bmatrix}\boldsymbol{a}_x(\phi,\theta)\\ \boldsymbol{a}_y(\phi,\theta)\end{bmatrix}\right)e^{(j\boldsymbol{\gamma}\cdot\boldsymbol{r})},\end{aligned} \tag{3}$$

where PL is the path loss, σ_{SF} is the log normal fading coefficients, and, K represents the Rician factor. $\boldsymbol{a}_x$ and $\boldsymbol{a}_y$ are the beamforming steering vector in x and y axes, respectively. ϕ represents the angle of azimuth while θ represents the elevation angle. In (3), $\boldsymbol{r}$ denotes the radial position of the MS and $\boldsymbol{\gamma}$ will be the angle of departure (AoD) for the BS and is given by

$$\boldsymbol{\gamma} = [\cos\phi\sin\theta, \sin\phi\sin\theta, \sin\phi]^T. \tag{4}$$

In case of a uniform planar array (UPA) with $N_t = N \times N$ elements, the response vector in x and y axes are given as [38]

$$\boldsymbol{a}_x(\phi,\theta) = \frac{1}{\sqrt{N}}[1, e^{j\beta_x}, \cdots, e^{j(N-1)\beta_x}]^T, \tag{5}$$

$$\boldsymbol{a}_y(\phi,\theta) = \frac{1}{\sqrt{N}}[1, e^{j\beta_y}, \cdots, e^{j(N-1)\beta_y}]^T, \tag{6}$$

where $0 \leq n < N$, β_x and β_y are the path differences along x and y axes, respectively. It can be observed that each of the above vectors consists of N entries, with each entry corresponding to an antenna element, given by

$$\beta_x = -2\pi\lambda^{-1}d_x\cos\phi\sin\theta, \tag{7}$$

$$\beta_y = -2\pi\lambda^{-1}d_y\sin\phi\sin\theta, \tag{8}$$

where dx and dy is the inter element spacing in x and y axes respectively. In our work, dx and dy are fixed at $\lambda/2$, where λ is the wavelength of the mmWave signal. For mmWave systems, higher frequencies will lead to smaller wavelengths and therefore more antennas elements can be packed for a given size. The array steering matrix is given by [39]

$$\boldsymbol{A} = \boldsymbol{a}_x(\phi,\theta) \otimes \boldsymbol{a}_y(\phi,\theta)^T. \tag{9}$$

If the 3D beampattern is generated using (5) and (6), unwanted side lobes will also be generated, radiating energy in unwanted directions. This will cause interference to users operating in the same area. KB filters have the capability of attenuating side lobes, and thus making the beampattern more directional. By introducing KB filters in the synthesis of the beampattern, side lobes can be decreased and directivity of the antenna can be improved. The KB filter is defined as [32]

$$\boldsymbol{z}_n = \begin{bmatrix}\frac{I_0(\mu\sqrt{(1-(\frac{2n}{N}-1))})}{I_0(\mu)}, & \text{if} \quad 0 \leq n \leq N-1\\ 0, & \text{Otherwise}\end{bmatrix}. \tag{10}$$

In (10), $I_0(\cdot)$ is the zeroth order modified Bessel function of the first kind and μ is the design parameter that is used to calculate the side lobe attenuation level. The array steering as defined in (5) and (6) are now combined with KB filters in (10), yielding

$$\boldsymbol{a}_x(\phi,\theta) = \frac{1}{\sqrt{N}}[z_1, z_2e^{j\beta_x}, \cdots, z_{N-1}e^{j(N-1)\beta_x}]^T, \tag{11}$$

$$\boldsymbol{a}_y(\phi,\theta) = \frac{1}{\sqrt{N}}[z_1, z_2e^{j\beta_y}, \cdots, z_{N-1}e^{j(N-1)\beta_y}]^T, \tag{12}$$

where $z_1, z_2, \cdots, z_n$ are the weights of the KB filter defined in (10).

III. Beamformer Design

In this section, two types of beamformers are considered for mmWave system. Initially, SVD approach is adopted to design the weights of the beamformer. Finally, the PSO algorithm is proposed. Further, to compare these algorithms, the antennas transmit power is kept the same by placing a constraint on beamforming matrix such that $|det(\boldsymbol{W}^H\boldsymbol{W})| = 1$. Moreover, if all the antenna elements are required to transmit at the same maximum power level, all diagonal elements of the matrix $\boldsymbol{W}\boldsymbol{W}^H$ must be identical. Therefore, the beamforming matrix $\boldsymbol{W}$ cannot be chosen freely and has to satisfy the following two constraints:

$\boldsymbol{I}$. $|det(\boldsymbol{W}^H\boldsymbol{W})| = 1$, i.e. (all) the algorithms have same transmitted power.
$\boldsymbol{II}$. $w_{mm} = \boldsymbol{W}\boldsymbol{W}^H(m,m) = \frac{1}{N}, m = 1, 2, \cdots, N$,
forcing the norm of each column of $\boldsymbol{W}$ to be equal to unity.

While the first constraint is specific to implementation of each algorithm, the general proof of the second constraint has been presented in Appendix A. Each algorithm is now discussed in details.

IV. Proposed approaches

A. Singular Value Decomposition (SVD)

In SVD beamforming, the channel matrix is factorized into singular values and unitary matrices. The SVD of the $N \times N$ matrix $\boldsymbol{H}$ is given by $\boldsymbol{H} = \boldsymbol{U}^H\boldsymbol{\Sigma}\boldsymbol{V}^H$ where $\boldsymbol{U}$ and $\boldsymbol{V}$ (also having dimensions of $N \times N$) are special matrices: a) They are unitary and hence $\boldsymbol{U}^H\boldsymbol{U} = \boldsymbol{V}^H\boldsymbol{V} = \boldsymbol{I}$; b) The columns of $\boldsymbol{U}$ and $\boldsymbol{V}$ are the eigen vectors of $\boldsymbol{H}\boldsymbol{H}^H$ and $\boldsymbol{H}^H\boldsymbol{H}$ respectively; c) The columns of $\boldsymbol{U}$ and $\boldsymbol{V}$ are also the orthonormal basis vectors of $\boldsymbol{H}\boldsymbol{H}^H$ and $\boldsymbol{H}^H\boldsymbol{H}$ respectively, and; d) $\boldsymbol{U}$ and $\boldsymbol{V}$ are orthogonal to each other as well. Lastly, $\boldsymbol{\Sigma} = diag[\sigma_1, \sigma_2, \cdots, \sigma_N]$ is an $N \times N$ diagonal matrix comprising of the N singular values of $\boldsymbol{H}$. These N singular values are the square root of the N eigen values of both $\boldsymbol{H}\boldsymbol{H}^H$ and $\boldsymbol{H}^H\boldsymbol{H}$. The weights of the SVD beamformer which maximizes the received SNR are formulated as

$$\boldsymbol{W} = \boldsymbol{V}\boldsymbol{\Sigma}^{-1}\boldsymbol{U} \tag{13}$$

This beamformer satisfies the constraint **I** as follows:

$$\begin{aligned} |det(\boldsymbol{W}^H\boldsymbol{W})| &= |det((\boldsymbol{V}\boldsymbol{\Sigma}^{-1}\boldsymbol{U})^H\boldsymbol{V}\boldsymbol{\Sigma}^{-1}\boldsymbol{U})| \\ &\overset{\mathbf{a}}{=} |det(\boldsymbol{U}^H\boldsymbol{\Sigma}^{-1}\underbrace{\boldsymbol{V}^H\boldsymbol{V}}_{\boldsymbol{I}:identity}\boldsymbol{\Sigma}^{-1}\boldsymbol{U})|, \overset{\mathbf{b}}{=} |det(\boldsymbol{U}^H\underbrace{\boldsymbol{\Sigma}^{-1}\boldsymbol{\Sigma}^{-1}}_{\boldsymbol{\Sigma}^{-2}}\boldsymbol{U})| \\ &\overset{\mathbf{c}}{=} |det(\boldsymbol{U}^H\boldsymbol{\Sigma}^{-2}\boldsymbol{U})|, \overset{\mathbf{d}}{=} |det(\boldsymbol{Z})| = 1 \end{aligned} \tag{14}$$

a: $(\boldsymbol{V}\boldsymbol{\Sigma}^{-1}\boldsymbol{U})^H = \boldsymbol{U}^H\boldsymbol{\Sigma}^{-1}\boldsymbol{V}^H$ and $(\boldsymbol{\Sigma}^{-1})^H = \boldsymbol{\Sigma}^{-1}$ because $\boldsymbol{\Sigma}^{-1}$ is an $N \times N$ diagonal matrix.
b: $\boldsymbol{V}^H\boldsymbol{V} = \boldsymbol{I}$, where $\boldsymbol{I}$ is the $N \times N$ identity matrix.
c: $\boldsymbol{\Sigma}^{-1}\boldsymbol{\Sigma}^{-1} = \boldsymbol{\Sigma}^{-2}$ because $\boldsymbol{\Sigma}^{-1}$ is an $N \times N$ diagonal matrix.
d: where $\boldsymbol{Z}$ is $N \times N$ an unitary matrix and unitary matrices have a determinant of unity.

The SNR achieved by the SVD beamformer weights formulated by (2) is given by

$$\begin{aligned} \text{SNR} &= \frac{|det[\boldsymbol{H}^H\boldsymbol{W}^H\boldsymbol{W}\boldsymbol{H}]|}{\sigma^2} \\ &\overset{\mathbf{a}}{=} \frac{|det[\boldsymbol{V}\boldsymbol{\Sigma}\overbrace{\boldsymbol{U}\boldsymbol{U}^H}^{\boldsymbol{I}}\boldsymbol{\Sigma}^{-2}\overbrace{\boldsymbol{U}\boldsymbol{U}^H}^{\boldsymbol{I}}\boldsymbol{\Sigma}\boldsymbol{V}^H]|}{\sigma^2}, \overset{\mathbf{b}}{=} \frac{|det[\boldsymbol{V}\overbrace{\boldsymbol{\Sigma}\boldsymbol{\Sigma}^{-2}\boldsymbol{\Sigma}}^{E_s}\boldsymbol{V}^H]|}{\sigma^2} \\ &\overset{\mathbf{c}}{=} \frac{E_s|det[\overbrace{\boldsymbol{V}\boldsymbol{V}^H}^{\boldsymbol{I}}]|}{\sigma^2}, \overset{\mathbf{d}}{=} \frac{E_s}{\sigma^2} \end{aligned} \tag{15}$$

a: $\boldsymbol{H}^H = (\boldsymbol{U}^H\boldsymbol{\Sigma}\boldsymbol{V}^H)^H = \boldsymbol{V}\boldsymbol{\Sigma}\boldsymbol{U}, \boldsymbol{W}^H\boldsymbol{W} = \boldsymbol{U}^H\boldsymbol{\Sigma}^{-2}\boldsymbol{U}$
b: $\boldsymbol{U}\boldsymbol{U}^H = \boldsymbol{I}$ because $\boldsymbol{U}$ is a unitary matrix.
c: $\boldsymbol{\Sigma}\boldsymbol{\Sigma}^{-2}\boldsymbol{\Sigma} = E_s$ where E_s was defined as the symbol power per time slot.
d: $det(\boldsymbol{V}\boldsymbol{V}^H) = 1$ because $\boldsymbol{V}$ is a unitary matrix, $\boldsymbol{V}\boldsymbol{V}^H = \boldsymbol{I}$ and $det(\boldsymbol{I} = 1)$.

It can be observed that the SVD algorithm requires the factorization of the 3D channel matrix. In this case, SVD algorithm still have similar computation complexity as that of finding the inverse of the received correlation matrix.

B. Particle Swarm Optimization (PSO)

This algorithm does not require any matrix inversion as in MVD or any matrix factorization as proposed in SVD. It assumes random weights and adaptively optimizes the weights that maximizes the SNR as shown in (2). The iterative steps in PSO algorithm are as follows:
Step 1. Initialize, P weights $\boldsymbol{W}_1(0), \boldsymbol{W}_2(0), \cdots, \boldsymbol{W}_p(0)$ with Gaussian random numbers. All weights will be of dimension $N \times N$. To force the constraint on the diagonal element $w_{mm} = \boldsymbol{W}\boldsymbol{W}^H(m,m) = 1$, every row of $\boldsymbol{W}_i(0)$ is divided by $\sqrt{\frac{1}{N}\sum_{n=1}^{N} w_{m,n}^2}$ where $1 \le m \le N$ is the mth row of $\boldsymbol{W}_i(0)$, and $1 \le n \le N$ is the nth column of $\boldsymbol{W}_i(0)$.
Step 2. Initialize the velocity of the i-th weight, $\boldsymbol{V}_i$, with a uniform random variable. The velocity will also be an $N \times N$ dimensional matrix.
Step 3. For each weight's position the value of the signal power is evaluated. The weight which gives the best signal power is found. This weight is denoted by $\boldsymbol{G}_{best} = \boldsymbol{W}_{best}$, and is the global best weight. Because the constraints **I** and **II** are enforced in Step 1, $|det(\boldsymbol{W}_{best}^H\boldsymbol{W}_{best})| = 1$ and $\boldsymbol{W}_{best}\boldsymbol{W}_{best}^H(m,m) = 1$.
Step 4. The velocity $\boldsymbol{V}_i$ and weights $\boldsymbol{W}_i$ of i-th weight are updated as

$$\begin{aligned} \boldsymbol{V}_i(\text{iter}+1) = {} & \boldsymbol{V}_i(\text{iter}) \\ & + c_1\text{rand}(L) \odot \left(\boldsymbol{W}^i_{\text{best}}(\text{iter}) - \boldsymbol{W}^i_{\text{current}}(\text{iter})\right) \\ & + c_2\text{rand}(L) \odot \left(\boldsymbol{G}_{\text{best}} - \boldsymbol{W}^i_{\text{current}}(\text{iter})\right), \end{aligned} \tag{16}$$

and the beamforming weight is given as

$$\boldsymbol{W}_i(\text{iter}+1) = \boldsymbol{W}_i(\text{iter}) + \boldsymbol{V}_i(\text{iter}+1). \tag{17}$$

In (19), $\boldsymbol{W}^i_{\text{best}}$ is the best and $\boldsymbol{W}^i_{\text{current}}$ is the current weight after the i-th iteration. The c_1 and c_2 are constants and their

values are kept close to 2. In the first iteration, $\boldsymbol{W}_{\text{best}}$ is considered equal to the $\boldsymbol{W}^i_{\text{current}}(0)$ for $i = 1, 2, 3, \cdots, P$. This step is repeated for each weight.

Step 5. Once the value of the i-th weight is updated its fitness is evaluated. If the updated fitness of the weight is less then the previous best-fitness of the weight then $\boldsymbol{W}^i_{\text{best}}(\text{iter}) = \boldsymbol{W}^i_{\text{current}}(\text{iter})$. **Step 6.** The best-weight, $\boldsymbol{W}_{\text{best}}$, whose fitness is the best fit signal power is found.

The SNR attained by the PSO algorithm can be obtained by substituting the global best weight $\boldsymbol{W}_{\text{best}}$ in (2).

V. Simulation Results

In this section, the simulation results are presented to validate the performance of our proposed algorithms when combined with KB filters. Initially, we plot the beam pattern of our system synthesized with and without KB filters. After that the capacity of the system per time slot versus the SNR per antenna element is measured when using PSO, SVD and MVD beamformers. In the simulations, the channel gains are assumed to follow the

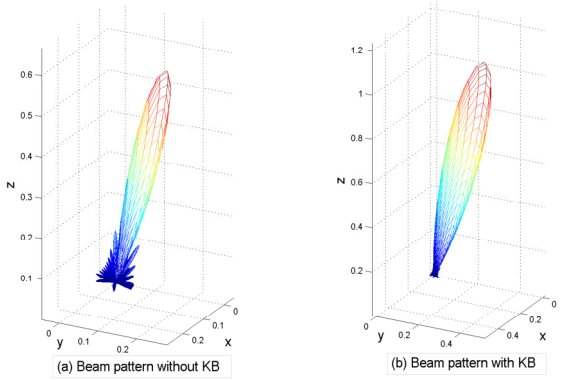

Figure 2: Comparison of beam pattern for $N_t = 16 \times 16$ antennas.

Fig. 2 plots the beam pattern of the system when synthesized with and without KB filter for $N_t = 16 \times 16$ antennas. The angle of azimuth ϕ is fixed to 45-degrees, while the elevation θ angle is 30-degrees. From the figure, it can be observed that when KB filters are not applied, there are strong side lobes. These side lobes will affect the received SNR of the system as a significant loss is observed in the gain of the synthesized beam pattern when comparing it with the system that adopts

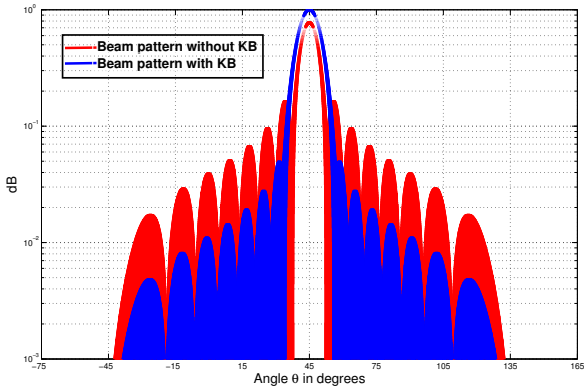

Figure 3: Beam pattern gain in dB with and without KB filters.

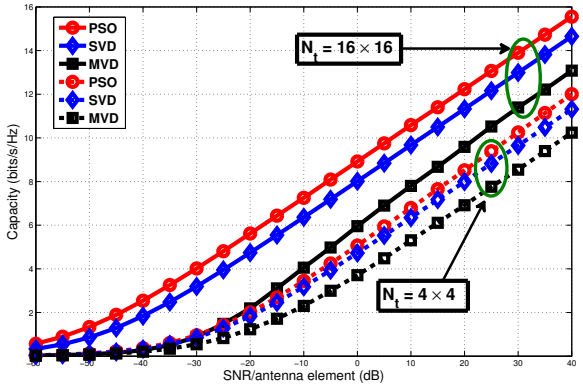

Figure 4: Capacity of the mmWave system with KB filters.

Fig. 3 compares the gain of the beam pattern in dB with and without KB filters. It can be clearly observed that while the system with KB filter not only achieves a higher gain in the main beam and hence higher beam directionality, the side lobes are also suppressed by at least an order of magnitude. This implies that the KB filter attenuates the side lobes by steering the energy from the side lobes into the main beam. These lower side lobes will help cause less interference .

Fig. 4 shows the capacity versus SNR of the mmWave system for all the algorithms with and without KB filters for $N_t = 16 \times 16$ antennas. It can be observed that with the application of KB filters, the capacity of the system improves. All these algorithms use the KB filters. It can be observed that the PSO and SVD beamformers attain higher capacity than MVD. This verifies the suboptimal nature of the MVD beamformer in the joint xy plane. Furthermore, PSO offering better performance of all.

VI. Conclusions

In this paper, two types of 3D beamforming algorithms were proposed for mmWave system. SVD was obtained by the factorizing the 3D channel into its unitary matrices and singular values, and PSO was an iterative algorithm that uses swarm optimization technique to obtain the global best solution. These beamformers can improve the capacity performance of a mmWave system when communicating over Rician fading channels. Due to the large number of antennas in the system, SVD approach has a high computational complexity. To reduce the computational complexity of SVD, another approach were proposed in this paper based on PSO. Furthermore KB filters are proposed for attaining high directionality and side lobe attenuation. From the simulations, it was observed that the PSO beamformer outperforms the SVD and MVD beamformers in terms of capacity. With the application of KB filters, a highly directional beam is attained and side lobes are also attenuated significantly.

Appendix A

The constraint $w_{mm} = \boldsymbol{W}\boldsymbol{W}^H(m,m) = \frac{1}{N}, m = 1, 2, \cdots, N$ in Section III can be proven as follows. The beamformer weights $\boldsymbol{W}$ are designed as

$$\boldsymbol{W} = [\frac{\boldsymbol{w}_{1n}}{N\sqrt{\sum_{n=1}^{N} w_{1n}^2}}, \frac{\boldsymbol{w}_{2n}}{N\sqrt{\sum_{n=1}^{N} w_{2n}^2}}, \cdots, \frac{\boldsymbol{w}_{N,n}}{N\sqrt{\sum_{n=1}^{N} w_{N,n}^2}}]^T, \quad (18)$$

where $\boldsymbol{w}_{1n}, \boldsymbol{w}_{2n}, \cdots, \boldsymbol{w}_{Nn}$ are the column vectors of $\boldsymbol{W}$. Therefore, the diagonal elements of the matrix $\boldsymbol{W}\boldsymbol{W}^H$ can be given by

$$\begin{aligned} diag[\boldsymbol{W}\boldsymbol{W}^H] = [&\frac{w_{11}w_{11}^* + w_{12}w_{12}^* + \cdots + w_{1N}w_{1N}^*}{w_{11}w_{11}^* + w_{12}w_{12}^* + \cdots + w_{1N}w_{1N}^*}, \\ &\frac{w_{21}w_{21}^* + w_{22}w_{22}^* + \cdots + w_{2N}w_{2N}^*}{w_{21}w_{21}^* + w_{22}w_{22}^H + \cdots + w_{2N}w_{2N}^*}, \\ &\cdots, \\ &\frac{w_{N1}w_{N1}^* + w_{N2}w_{N2}^* + \cdots + w_{NN}w_{NN}^*}{w_{N1}w_{N1}^* + w_{N2}w_{N2}^* + \cdots + w_{NN}w_{NN}^*}] \end{aligned} \quad (19)$$

or $diag[\boldsymbol{W}\boldsymbol{W}^H] = [1, 1, \cdots, 1]$

REFERENCES

[1] C. Pan, H. Zhu, N. J. Gomes, and J. Wang, "Joint Precoding and RRH Selection for User-Centric Green MIMO C-RAN," *IEEE Trans. on Wireless Commun.*, vol. 16, no. 5, pp. 2891–2906, May 2017.

[2] J. Wang, H. Zhu, and N. J. Gomes, "Distributed Antenna Systems for Mobile Communications in High Speed Trains," *IEEE J. Sel. Areas in Commun.*, vol. 30, no. 4, pp. 675–683, May. 2012.

[3] H. Zhu, "Performance Comparison Between Distributed Antenna and Microcellular Systems," *IEEE J. Sel. Areas in Commun.*, vol. 29, no. 6, pp. 1151–1163, Jun. 2011.

[4] J. Wang, H. Zhu, L. Dai, N. J. Gomes, and J. Wang, "Low-Complexity Beam Allocation for Switched-Beam Based Multiuser Massive MIMO Systems," *IEEE Trans. on Wireless Communi.*, vol. 15, no. 12, pp. 8236–8248, Dec 2016.

[5] H. Zhu and J. Wang, "Chunk-based resource allocation in OFDMA systems - part I: chunk allocation," *IEEE Transactions on Com.*, vol. 57, no. 9, pp. 2734–2744, Sep. 2009.

[6] D. Love, R. Heath, and T. Strohmer, "Grassmannian beamforming for multiple-input multiple-output wireless systems," *IEEE Transactions on Information Theory*, vol. 49, no. 10, pp. 2735–2747, Oct 2003.

[7] T. Do-Hong and P. Russer, "A new design method for digital beamforming using spatial interpolation," *IEEE Antennas and Wireless Propagation Letters*, vol. 2, no. 1, pp. 177–181, 2003.

[8] H. Zhu and J. Wang, "Performance Analysis of Chunk-Based Resource Allocation in Multi-Cell OFDMA Systems," *IEEE Journal on Selected Areas in Com.*, vol. 32, no. 2, pp. 367–375, Feb. 2014.

[9] ——, "Radio Resource Allocation in Multiuser Distributed Antenna Systems," *IEEE Journal on Selected Areas in Com.*, vol. 31, no. 10, pp. 2058–2066, Oct. 2013.

[10] H. Osman, H. Zhu, D. Toumpakaris, and J. Wang, "Achievable Rate Evaluation of In-Building Distributed Antenna Systems," *IEEE Transactions on Wireless Com.*, vol. 12, no. 7, pp. 3510–3521, Jul. 2013.

[11] T. Alade, H. Zhu, and J. Wang, "Uplink Spectral Efficiency Analysis of In-Building Distributed Antenna Systems," *IEEE Transactions on Wireless Com.*, vol. 14, no. 7, pp. 4063–4074, Jul. 2015.

[12] H. Zhu, S. Karachontzitis, and D. Toumpakaris, "Low-complexity resource allocation and its application to distributed antenna systems [Coordinated and Distributed MIMO]," *IEEE Wireless Communications*, vol. 17, no. 3, pp. 44–50, Jun. 2010.

[13] H. Zhu, "On frequency reuse in cooperative distributed antenna systems," *IEEE Communications Magazine*, vol. 50, no. 4, pp. 85–89, Apr. 2012.

[14] H. Zhu, B. Xia, and Z. Tan, "Performance Analysis of Alamouti Transmit Diversity with QAM in Imperfect Channel Estimation," *IEEE Journal on Selected Areas in Communications*, vol. 29, no. 6, pp. 1242–1248, Jun. 2011.

[15] Q. Z. Ahmed, K. H. Park, M. S. Alouini, and S. Aissa, "Linear Transceiver Design for Nonorthogonal Amplify-and-Forward Protocol Using a Bit Error Rate Criterion," *IEEE Transactions on Wireless Com.*, vol. 13, no. 4, pp. 1844–1853, Api. 2014.

[16] Y. Xin, D. Wang, J. Li, H. Zhu, J. Wang, and X. You, "Area spectral efficiency and area energy efficiency of massive mimo cellular systems," *IEEE Transactions on Vehicular Technology*, vol. 65, no. 5, pp. 3243–3254, May 2016.

[17] H. Wei, D. Wang, H. Zhu, J. Wang, S. Sun, and X. You, "Mutual coupling calibration for multiuser massive mimo systems," *IEEE Transactions on Wireless Communications*, vol. 15, no. 1, pp. 606–619, Jan 2016.

[18] A. Alkhateeb, J. Mo, N. Gonzalez-Prelcic, and R. Heath, "MIMO precoding and combining solutions for millimeter-wave systems," *IEEE Communications Magazine*, vol. 52, no. 12, pp. 122–131, December 2014.

[19] G. Zhu, K. Huang, V. K. N. Lau, B. Xia, X. Li, and S. Zhang, "Hybrid Beamforming via the Kronecker Decomposition for the Millimeter-Wave Massive MIMO Systems," *IEEE J. Sel. Areas in Commun.*, vol. PP, no. 99, pp. 1–1, Jun. 2017.

[20] O. Alluhaibi, Q. Z. Ahmed, J. Wang, and H. Zhu, "Hybrid digital-to-analog precoding design for mm-wave systems," in *2017 IEEE International Conference on Communications (ICC)*, May 2017, pp. 1–6.

[21] O. Alluhaibi, Q. Z. Ahmed, C. Pan, and H. Zhu, "Capacity Maximisation for Hybrid Digital-to-Analog Beamforming mm-Wave Systems," in *2016 IEEE Global Communications Conference (GLOBECOM)*, Dec 2016, pp. 1–6.

[22] ——, "Hybrid Digital-to-Analog Beamforming Approaches to Maximise the Capacity of mm-Wave Systems," in *2017 IEEE 85th Vehicular Technology Conference (VTC Spring)*, June 2017, pp. 1–5.

[23] E. C. Cejudo, H. Zhu, and O. Alluhaibi, "On the Power Allocation and Constellation Selection in Downlink NOMA," in *2017 IEEE 86th Vehicular Technology Conference (VTC-Fall)*, Sept 2017, pp. 1–5.

[24] O. Alluhaibi and Q. Z. Ahmed, "Multi-User Hybrid Precoding and Decoding Design for mm-Wave Large Antenna Systems," in *2018 IEEE 87th Vehicular Technology Conference (VTC Spring)*, June 2018, pp. 1–5.

[25] S. Sun, T. Rappaport, R. Heath, A. Nix, and S. Rangan, "MIMO for millimeter-wave wireless communications: beamforming, spatial multiplexing, or both," *IEEE Communications Magazine*, vol. 52, no. 12, pp. 110–121, December 2014.

[26] S. Hur, T. Kim, D. Love, J. Krogmeier, T. Thomas, and A. Ghosh, "Millimeter wave beamforming for wireless backhaul and access in small cell networks," *IEEE Transactions on Communications*, vol. 61, no. 10, pp. 4391–4403, October 2013.

[27] J. Wang, Z. Lan, C.-W. Pyo, T. Baykas, C.-S. Sum, M. Rahman, J. Gao, R. Funada, F. Kojima, H. Harada, and S. Kato, "Beam codebook based beamforming protocol for multi-Gbps millimeter-wave WPAN systems," *IEEE Journal on Selected Areas in Communications*, vol. 27, no. 8, pp. 1390–1399, October 2009.

[28] M. Crocco and A. Trucco, "Design of Superdirective Planar Arrays With Sparse Aperiodic Layouts for Processing Broadband Signals via 3-D Beamforming," *IEEE/ACM Transactions on Audio Speech and Language Processing*, vol. 22, no. 4, pp. 800–815, April 2014.

[29] Z. Hu, R. Liu, S. Kang, X. Su, and J. Xu, "Work in progress: 3D beamforming methods with user-specific elevation beamfoming," in *9th International Conference on Communications and Networking in China*, Aug 2014, pp. 383–386.

[30] E. Santos, M. Zoltowski, and M. Rangaswamy, "Indirect dominant mode rejection: A solution to low sample support beamforming," *IEEE Transactions on Signal Processing*, vol. 55, no. 7, pp. 3283–3293, July 2007.

[31] K. Kim, S. Park, J. Kim, S.-B. Park, and M. Bae, "A fast minimum variance beamforming method using principal component analysis," *IEEE Transactions on Ultrasonics, Ferroelectrics, and Frequency Control*, vol. 61, no. 6, pp. 930–945, June 2014.

[32] F. B. Gross, "Smart antenna for wireless communication with MATLAB," *McGraw-Hill New York*, June 2005.

[33] M. Dong, W. Chan, T. Kim, K. Liu, H. Huang, and G. Wang, "Simulation study on millimeter wave 3D beamforming systems in urban outdoor multi-cell scenarios using 3D ray tracing," in *2015 IEEE 26th Annual International Symposium on Personal, Indoor, and Mobile Radio Communications (PIMRC)*, Aug 2015, pp. 2265–2270.

[34] C.-C. Chou and J.-M. Wu, "Low-complexity MIMO precoder design with channel decomposition," *IEEE Transactions on Vehicular Technology*, vol. 60, no. 5, pp. 2368–2372, Jun 2011.

[35] S.-H. Park, H. Lee, S.-R. Lee, and I. Lee, "A new beamforming structure based on transmit-MRC for closed-loop MIMO systems," *IEEE Transactions on Communications*, vol. 57, no. 6, pp. 1847–1856, June 2009.

[36] A. Kammoun, H. Khanfir, Z. Altman, M. Debbah, and M. Kamoun, "Preliminary results on 3D channel modeling: from theory to standardization," *IEEE Journal on Selected Areas in Communications*, vol. 32, no. 6, pp. 1219–1229, June 2014.

[37] B. Mondal, T. Thomas, E. Visotsky, F. Vook, A. Ghosh, Y. han Nam, Y. Li, J. Zhang, M. Zhang, Q. Luo, Y. Kakishima, and K. Kitao, "3D channel model in 3GPP," *IEEE Communications Magazine*, vol. 53, no. 3, pp. 16–23, March 2015.

[38] O. El Ayach, S. Rajagopal, S. Abu-Surra, Z. Pi, and R. Heath, "Spatially sparse precoding in millimeter wave MIMO systems," *IEEE Transactions on Wireless Communications*, vol. 13, no. 3, pp. 1499–1513, March 2014.

[39] Y. Han, S. Jin, X. Li, Y. Huang, L. Jiang, and G. Wang, "Design of double codebook based on 3D dual-polarized channel for multiuser MIMO system," *EURASIP Journal on Advances in Signal Processing*, vol. 2014, no. 1, July 2014.